# A Novel $S = {}^7/_2$ Configuration of the Mn Cluster of Photosystem II

Yiannis Sanakis,[†,‡] Nikolaos Ioannidis,[†] George Sioros,[†] and Vasili Petrouleas*[,†]

*Institute of Materials Science, NCSR "Demokritos" 153 10 Aghia Paraskevi Attikis, Greece*
*Department of Biological Applications and Technologies University of Ioannina, 45110 Ioannina, Greece*

*Received June 14, 2001*

The oxygen evolving complex (OEC) of Photosystem II (PSII) comprises a tetranuclear Mn cluster, a redox-active tyrosine, Z, and the cofactors $Ca^{2+}$ and $Cl^-$.[1] The OEC cycles through five redox states denoted $S_i$, $i = 0, 1, 2, 3, 4$, as it undergoes consecutive one-electron oxidations by a photooxidizable chlorophyll species termed $P_{680}$. Upon accumulation of four oxidizing equivalents ($S_4$ state), two water molecules are oxidized, molecular oxygen is expelled, and the cycle starts again ($S_0$ state). EPR spectroscopy has been crucial in the characterization of the various S-states. A recent advance is the detection of EPR signals in both perpendicular and parallel mode from the $S_3$ state.[2,3] Interestingly, the OEC poised at this state was found to be sensitive to near-infrared (NIR) light[3] in a fashion similar to that of the $S_2$-state.[4]

NIR excitation of $S_3$ produces among other changes a prominent EPR signal at about $g \sim 5$.[3] This is illustrated in Figure 1A. Spectra A1 and A2 represent the $S_3$-state prior and after the NIR illumination at 50 K. Their difference shown in Figure 1A clearly demonstrates the induction of a derivative signal at $g = 4.65$, as well as a broader derivative at $g = 3$. The $g = 4.65$ signal shows an interesting similarity to the, so-called, $g = 5$ signal obtained earlier by Nugent et al.[5] after prolonged incubation at 77 K of samples that had undergone multiple turnovers from the $S_1$ state. We have confirmed the observations of Nugent et al.[5] with samples poised at the $S_3$ state. Spectrum B1 in Figure 1 shows the spectrum of a sample poised at $S_3$ (initial spectrum similar to spectrum A1) and incubated at 77 K for several weeks. The spectrum shows a pronounced derivative signal at $g \sim 5$, partially distorted by background contributions. Upon warming to −50 °C for 2 min, spectrum B2, the signal loses considerable intensity. By subtracting the two spectra, Figure 1B, a derivative signal with a zero crossing point at $g = 4.75$ is obtained.

Spectra A and B in Figure 1 contain similar signals at $g \sim 5$ except that in spectrum A the signal is broader and the $g$ value is shifted to smaller values.[6] Spectrum A contains in addition a broad derivative contribution at about $g = 3$. Annealing of the sample in spectrum A for a few minutes at 77 K results in a decrease of the $g = 3$ feature and a narrowing of the $g \sim 5$ signal, i.e., a shift toward spectrum B (not shown). The treatments that induce

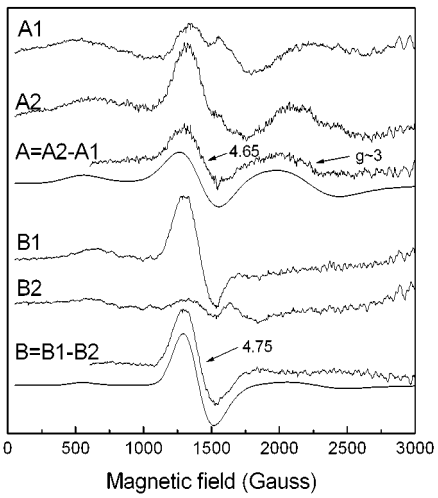


**Figure 1.** Changes to the EPR spectra of PSII samples poised at the $S_3$ state, A1, induced by N.I.R. irradiation at 50 K, A2, or by prolonged incubation at 77 K, B1, and subsequent 2 min annealing at −50 °C, B2. The background spectrum of $S_1$ has been subtracted. Noiseless traces are theoretical simulations of the difference spectra, A and B, assuming an $S = {}^7/_2$ state (see text). PSII-enriched thylakoid membranes were suspended in 0.4 M sucrose, 15 mM NaCl, 40 mM MES, pH 6.5, at 6−8 mg Chl/mL (5 mm EPR tubes). EPR conditions (Bruker ER-200D upgraded): microwave frequency 9.385 *GHz*, temperature 4.2 K, mod. ampl. 25 $G_{pp}$, microwave power 32 mW.

(Figure A2) or diminish (Figure B2) the $g \sim 5$ signal inevitably affect the $S_3$-state signal at $g \sim 10$. As a result, the low-field region of spectra A and B is distorted and was omitted. This should be kept in mind when comparing with the theoretical spectra below.

For the analysis of the spectra in Figure 1 we assume a half-integer spin, $S > {}^1/_2$, in the context of the spin-Hamiltonian,

$$H = D[S_z^2 - S(S+1)/3] + E(S_x^2 - S_y^2) + \beta \mathbf{B} \mathbf{g_0} \mathbf{S} \quad (1)$$

The simplicity of the spectra suggests a zero-field splitting larger than the microwave energy, otherwise inter-doublet transitions would produce a multitude of peaks. The key feature of the spectra in Figure 1 is the derivative feature in the $g \sim 5$ region. We have diagonalized numerically (1) for various spin values and a first general conclusion is that resonances in the $g \sim 5$ region can be contributed only by the $|\pm{}^1/_2\rangle$, $|\pm{}^3/_2\rangle$ Kramer's doublets[7] for $E/D > 0$.[8] The $|\pm{}^1/_2\rangle$ doublet in general gives rise to anisotropic $g$ tensors with potential derivative features in the $g \sim 5$ region, but these are accompanied by strong absorption peaks at higher $g$ values, which are not observed here. The $g \sim 5$ signal, particularly in spectrum B, appears nearly isotropic. This explains its high intensity relative to anisotropic signals of PSII,[3,5] although an examination of the conditions for its production indicates that it represents a small fraction of centers, about 10−15% (spectrum A) or 20−25% (spectrum B).[9] Isotropic signals can result only from the $|\pm{}^3/_2\rangle$ doublet of any $S \geq {}^5/_2$ system, and only for a single $E/D$ value in each case. The zero crossing point of the

* E-mail: vpetr@ims.Demokritos.gr.
† NCSR "Demokritos".
‡ University of Ioannina.

(1) For reviews see: (a) Britt, R. D. In *Advances in Photosynthesis: Oxygenic Photosynthesis: The Light Reactions*; Ort, R. D., Yocum, C. F., Eds.; Kluwer Academic Publishers: Dordrecht, The Netherlands, 1996; Vol. 4, pp 137−164. (b) *Bioenergetics, Special Issue: Photosynthetic water oxidation*; Nugent, J., Guest Editor: *Biochim. Biophys. Acta* **2001**, *1503*.

(2) Matsukawa, T.; Mino, H.; Yoneda, D.; Kawamori, A. *Biochemistry* **1999**, *38*, 4072−4077.

(3) Ioannidis, N.; Petrouleas, V. *Biochemistry* **2000**, *39*, 5246−5254.

(4) Boussac, A.; Un, S.; Horner, O.; Rutherford, A. W. *Biochemistry* **1998**, *37*, 4001−4007.

(5) Nugent, J. H. A.; Turconi, S.; Evans, M. C. W. *Biochemistry* **1997**, *36*, 7086−7096.

(6) Similar NIR-induced $g \sim 5$ signals have been reported for the cyanobacterium *Synechococcus elongatus*: Boussac, A.; Sugiura, M.; Inoue, Y.; Rutherford, A. W. *Biochemistry* **2000**, *39*, 13788−13799. We have also observed both $g \sim 5$ signals in *Synechococcus vulcanus* in collaboration with J.-R. Shen and A. Kawamori (unpublished results).

(7) For simplicity we use $\pm m_s$ to label the doublets although $m_s$ is not a good quantum number for $E/D \neq 0$.

(8) In an extreme case the $g \sim 5$ could be an axial signal. The $g_\perp = 6.0$ resonance for an $S = {}^5/_2$ system shifts to $g = 4.75$ for $D = 0.175$ cm$^{-1}$. See e.g.: Pilbrow, J. R. *J. Magn. Reson.* **1978**, *31*, 479−490. However, inter-doublet transitions (absent in our spectra) are predicted in this case.

(9) Ioannidis, N.; Sanakis, Y.; Sioros, G.; Petrouleas, V. In preparation. The $g = 5$ configuration represents the sole decay product of the $S_3$ state at 77 K and can be trapped in significant amounts under optimal conditions.

10.1021/ja016418u CCC: $20.00 
Published on Web 10/04/2001

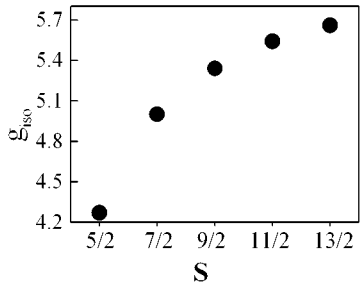


**Figure 2.** Dependence of $g_{iso}$ from the $|\pm^3/_2\rangle$ doublet[7] on the value of the spin for $D \gg |g_0B\beta|$ and $g_0 = 2.0$.

signal, $g_{iso}$, is spin dependent. This is demonstrated in Figure 2 where we plot the $g_{iso}$ from the $|\pm^3/_2\rangle$ doublet for spin values up to $^{13}/_2$.

The zero-crossing point of the $g \sim 5$ signals in Figure 1 at $g$ 4.6−4.8 lies between the $g_{iso}$ values expected for $S = {}^5/_2$ and ${}^7/_2$. Assuming that the free ion $g$ value is not substantially different than 2, this can be attributed to $E/D$ somewhat smaller than the isotropic value combined with spectral broadening.[10] This would cause a decrease of the phenomenological $g_{iso}$. Accordingly, the obvious spin choice from Figure 2 is ${}^7/_2$.

The $g$-value diagram for $S = {}^7/_2$ is shown as a function of $E/D$ in Figure 3. We also plot a series of theoretical spectra[11] for two different values of $D$ and a range of $E/D$ values in the vicinity of the isotropic value, which is 0.12 in this case. The values of $D$ were chosen based on a rough comparison of the unsaturated spectra at 4 K with their counterparts at 11 K (not shown) assuming Boltzmann statistics. The 11 K spectra are weak and masked by the $g = 4.1$ $S_2$-state signal, but an upper limit of their intensity could be estimated. The experimental spectra have been superimposed on the theoretical ones.

The spectra in Figure 3 clearly show the trend of the decreasing "$g_{iso}$" with decreasing $E/D$, and an accompanying increase of the width of the $g \sim 5$ signal. The spectra contain also weak contributions at $g \sim 12$ (peak) and in the 2000 to 3000$G$ region (derivative) from the $|\pm^1/_2\rangle$ doublet. Notable is the strong dependence of the position of the latter derivative on $E/D$. A similar feature at $g \sim 3$ is present in the experimental spectrum A.[12] The intensity of the "g ~ 3" and $g \sim 12$ resonances decreases as the thermal population of the $|\pm^1/_2\rangle$ doublet decreases with decreasing positive $D$. The absence of a discernible "$g = 3$" resonance in spectrum B is compatible with a smaller $D$ relative to spectrum A, as suggested by the temperature dependence.

Extension of the simulations combined with a fitting procedure yielded the theoretical spectra in Figure 1. Spectrum A is simulated with $D = 2$ cm$^{-1}$, $E/D = 0.095$, $\sigma_{E/D} = 0.005$, and $\sigma_B = 110$ $G$, while spectrum B is simulated with $D = +0.44$ cm$^{-1}$, $E/D = 0.103$, $\sigma_{E/D} = 0.007$ and $\sigma_B = 90$ $G$. The simulations are very satisfactory and support the present analysis.

Work in preparation examines the changes accompanying the NIR excitation of the $S_3$ state. It is argued that the NIR excitation

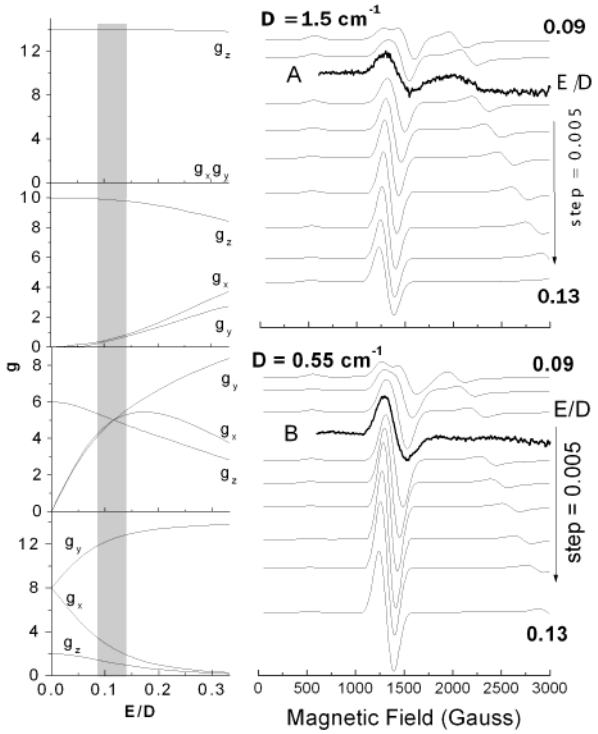


**Figure 3.** $g$-value diagram (as a function of $E/D$) for an $S = {}^7/_2$ state and theoretical spectra[11] for $E/D$ values in the isotropic region, and two representative values of $D$ ($\sigma_B = 70$ G, $\sigma_{E/D} = 0$). The experimental spectra A and B of Figure 1 were superimposed for comparison.

at low temperatures, by producing tyr $Z^+$ as an intermediate, speeds up charge recombination, and converts $S_3$ to a modified $S_2$ ($S = {}^7/_2$ ground-state), which would built up slowly during dark storage at 77 K.[9] This new spin state—highest spin detected so far in the Mn cluster and a rare (if detected at all) state in Mn complexes in general—is to be added to the three alternative configurations of $S_2$: the multiline ($S = {}^1/_2$),[13] the various "$g = 4.1$" signals (recent evidence favors $S = {}^5/_2$ over ${}^3/_2$)[14] and the $g = 10$, 6 (most likely $S = {}^5/_2$)[4] induced by NIR excitation of the multiline state. The $S = {}^7/_2$ state[15] is observed in both spinach and cyanobacterial preparations,[6] and appears to be a physiological intermediate during the decay of $S_3$. The different crystal field parameters describing spectra A and B mark early fine changes within the $S = {}^7/_2$ manifold. Whether this reflects a remote influence of tyr Z[16] will be examined in a future investigation.

**Acknowledgment.** We thank Dr. M. Hendrich (Carnegie Mellon Univ.) for providing us with the EPR simulation program. This work was supported by the Greek Secretariat of Research and Technology (PENED 99ED75).

JA016418U

(10) A significant source of broadening in addition to crystal field heterogeneities is the unresolved hyperfine interactions from the $^{55}$Mn nuclei, $I = {}^5/_2$. We considered a mixed-valence Mn cluster and adopted simple coupling schemes that produce $S = {}^7/_2$. The projected hyperfine tensors, $A_i$, fell in the range 55−80 MHz. Four $I = {}^5/_2$ nuclei with $A_i$ values in this range result in line widths comparable to the observed ones.

(11) Spectra were calculated by diagonalization of (1) and polycrystalline summation. The line shape was modeled with a homogeneous spin-packet line width of $\sigma_B$, and a Gaussian distribution in $E/D$ of width $\sigma_{E/D}$.

(12) A small distribution in $E/D$ in combination with the inherent broadening of the lines with smaller $g$-values (see: Pilbrow, J. R. *J. Magn. Reson.* **1984**, *58*, 186−203), which is taken into account in the simulation program, leads to a relatively large width of this feature.

(13) Dismukes, G. C.; Siderer, Y. *Proc. Natl. Acad. Sci. U.S.A.* **1981**, *78*, 274−278.

(14) For a recent study unifying the various $g = 4$ signals and their spin assignments see: Boussac, A.; Rutherford, A. W. *Biochim. Biophys. Acta* **2000**, *44832*, 1−12.

(15) Interestingly, the trimer/monomer model of Peloquin et al. predicts a change from a $S = {}^1/_2$ to a $S = {}^5/_2$ or ${}^7/_2$ ground state when the sign of the trimer to the monomer exchange constant changes: Peloquin, J. M.; Cambell, K. A.; Randall, D. W.; Evanchik, M. A.; Pecoraro, V. L.; Armstrong, W. H.; Britt, R. D. *J. Am. Chem. Soc.* **2000**, *122*, 10926−10942.

(16) The influence of tyr Z on the configuration of the Mn cluster has been suggested e.g. in the case of the acetate inhibited $S_2Z^+$ state: Szalai, V. A.; Kuhne, H.; Lakhsmi, K. V.; Brudvig, G. W. *Biochemistry* **1998**, *37*, 13594−13603.